IEEE Access
Multidisciplinary | Rapid Review | Open Access Journal

Received July 5, 2017, accepted August 1, 2017, date of publication August 9, 2017, date of current version September 19, 2017.

Digital Object Identifier 10.1109/ACCESS.2017.2737330

On Secure NOMA Systems With Transmit Antenna Selection Schemes

HONGJIANG LEI[1,2], (Member, IEEE), JIANMING ZHANG[1], KI-HONG PARK[2], (Member, IEEE), PENG XU[1], IMRAN SHAFIQUE ANSARI[3], (Member, IEEE), GAOFENG PAN[4], (Member, IEEE), BASEL ALOMAIR[5], (Member, IEEE), AND MOHAMED-SLIM ALOUINI[2], (Fellow, IEEE)

[1]Chongqing Key Lab of Mobile Communications Technology, Chongqing University of Posts and Telecommunications, Chongqing 400065, China
[2]Computer, Electrical, and Mathematical Sciences and Engineering Division, King Abdullah University of Science and Technology, Thuwal 23955-6900, Saudi Arabia
[3]Department of Electrical and Computer Engineering, Texas A&M University at Qatar, Education City, Doha 23874, Qatar
[4]School of Computing and Communications, Lancaster University, Lancashire LA1 4WA, U.K.
[5]National Center for Cybersecurity Technology, King Abdulaziz City for Science and Technology, Riyadh 11442, Saudi Arabia

Corresponding author: Hongjiang Lei (leihj@cqupt.edu.cn)

This work was supported in part by the National Natural Science Foundation of China under Grant 61471076, in part by the Chinese Scholarship Council under Grant 201607845004, in part by the Program for Changjiang Scholars and Innovative Research Team in University under Grant IRT_16R72, in part by the special fund for the Key Lab of Chongqing Municipal Education Commission, in part by the Project of Fundamental and Frontier Research Plan of Chongqing under Grant cstc2015jcyjBX0085 and Grant cstc2017jcyjAX0204, in part by the Scientific and Technological Research Program of Chongqing Municipal Education Commission under Grant KJ1600413 and Grant KJ1704088, and in part by the Qatar National Research Fund (a member of Qatar Foundation) under Grant NPRP7-125-2-061.

ABSTRACT This paper investigates the secrecy performance of a two-user downlink non-orthogonal multiple access systems. Both single-input and single-output and multiple-input and single-output systems with different transmit antenna selection (TAS) strategies are considered. Depending on whether the base station has the global channel state information of both the main and wiretap channels, the exact closed-form expressions for the secrecy outage probability (SOP) with suboptimal antenna selection and optimal antenna selection schemes are obtained and compared with the traditional space-time transmission scheme. To obtain further insights, the asymptotic analysis of the SOP in high average channel power gains regime is presented and it is found that the secrecy diversity order for all the TAS schemes with fixed power allocation is zero. Furthermore, an effective power allocation scheme is proposed to obtain the non-zero diversity order with all the TAS schemes. Monte Carlo simulations are performed to verify the proposed analytical results.

INDEX TERMS Non-orthogonal multiple access, physical layer security, transmit antenna selection, secrecy outage probability.

I. INTRODUCTION

A. BACKGROUND AND RELATED WORKS

Recently, non-orthogonal multiple access (NOMA) has been accepted as a potential technology for the fifth generation (5G) mobile networks in face of the explosive growth of the mobile traffic demands [1]–[4]. As opposed to the conventional orthogonal multiple access (OMA) technologies (e.g. time/frequency/code division multiple access), NOMA can substantially improve the spectral efficiency by accommodating multiple users simultaneously via power domain multiplexing. For example, in a downlink NOMA system that consists of a near user (that has high channel gain), a far user (that has low channel gain), and a base station. The base station transmits signals to both users simultaneously using superposition coding [5] and more transmission power is allocated to the far user. Under NOMA scheme, the near user decodes the signal to the far user first and then decodes its signal after subtracting the decoded signal to the far user by adopting successive interference cancellation (SIC). The signal to the far user can be decoded without significant interference from the signal to the near user, which is weak. The outage probability and ergodic capacity of NOMA system were studied in [6] when the users are randomly distributed in the vicinity of the base station, and confirmed that the performance of NOMA was significantly superior to the traditional OMA when the power allocation scheme was used. NOMA can also make the radio resources allocation more flexible, as well as can improve the user's fairness by employing appropriate resource allocation schemes [7]–[11]. As a promising candidate for 5G wireless networks, the integration

of NOMA and conventional OMA paradigms also plays an indispensable role in avoiding strong co-channel interference caused by serving multiple users at the same time, frequency, and spreading code [12], [13].

Recently, multiple-antenna technology has been utilized in NOMA systems to improve the system performance [14]-[18]. It was demonstrated that the sum rate of a multiple-input multiple-output (MIMO) NOMA system is strictly larger than that of a MIMO OMA system in [15]. The outage performance of NOMA system with a multiple-antenna energy harvesting relay was analyzed in [16]. Although the performance can potentially scale up with the number of antennas, the improvement comes at the price of expensive RF chains at the terminal. To avoid the high hardware costs while preserving the diversity and throughput benefits from multiple antennas, transmit antenna selection (TAS) technique has been recognized as an effective solution [16]–[18]. Due to the efficiency and flexibility, NOMA can also be combined with many other wireless technologies to enhance the system performance, such as cooperative communication [19], [20], full duplex [21], cognitive radio (CR) [22], millimeter wave [23], and visible light communication [24], etc.

Physical layer security has taken one of the hottest spots in both information security and wireless communications as it can realize the secrecy communication by utilizing the randomness and time-varying nature of the wireless channels without any encryption algorithm [25]. Zhang *et al*. studied the security performance of single-input-single-output (SISO) NOMA system, and confirmed that the secrecy sum rate performance of NOMA outperforms the one of the conventional OMA [26]. Qin *et al.* studied the physical layer security of NOMA systems in large-scale networks wherein both NOMA users and eavesdroppers are spatially deployed at randomly location [27], and new exact and asymptotic expressions for the secrecy outage probability (SOP) were derived. Furthermore, the secrecy performance of multiple-antenna NOMA with artificial noise was investigated and the exact and asymptotic expressions for SOP were derived in [28]. Depending on whether the base station has the global channel state information (CSI) of both the main and wiretap channels, Zhu *et al.* proposed optimal antenna selection (OAS) and suboptimal antenna selection (SAS) schemes to enhance the secrecy performance of a MIMO system in [29], which was compared with the traditional space-time transmission (STT) scheme. The closed-form expressions for the exact and asymptotic SOP of an underlay MIMO system were derived in [30]. The obtained results showed that both SAS and OAS schemes can significantly enhance the secrecy performance. Now we are wondering about the secrecy performance of these TAS schemes in NOMA system.

B. MOTIVATION AND CONTRIBUTIONS

Based on the open literature and to the best of the authors' knowledge, it is still an open issue to study the secrecy performance of multiple-input single-output (MISO) NOMA systems with TAS schemes. The main contributions of our work are listed as follows:

1) We investigate the secrecy outage performance of MISO NOMA system consisting of one base station with multiple antennas, two legitimate receivers, and an eavesdropper. We investigate the secrecy outage performance of OAS and SAS schemes for MISO NOMA system and compare them with the STT scheme. The closed-form expressions for the exact and asymptotic SOP are derived. Moreover, the accuracy of the analytical results are validated via Monte-Carlo simulations. The results show that the SOP for the far user with fixed power allocation scheme deteriorates as the transmit power surpasses some threshold and then reaches a floor as the interference from the near user increases while increasing the transmit power.
2) To obtain further insights, the asymptotic analysis of SOP is conducted and the secrecy diversity order for different TAS schemes is derived when the average signal-to-noise ratio (SNR) of the main channel tends to infinity. The results show that the secrecy diversity order for all the TAS schemes with fixed power allocation are zero.
3) Moreover, an effective power allocation scheme is proposed to obtain non-zero diversity order under all the TAS schemes. Simulations and numerical results are given to validate the accuracy of all the analytical results.

The rest of this paper is organized as follows. In Section II, the two-user NOMA system model is described. The performance analysis of SOP in a SISO NOMA system is carried out in Section III. In Sections IV and V the exact and asymptotic SOP in TAS-based MISO NOMA system are investigated. An effective power allocation method is proposed in Section VI and the secrecy diversity order for all the cases with proposed power allocation scheme is derived. Section VII presents and discusses the numerical results. Finally, we conclude the paper in Section VIII.

II. SYSTEM MODEL

In this work, we consider a downlink NOMA system that includes a base station (S), two legitimate users D_1 (the near user) and D_2 (the far user), and an eavesdropper (E), as shown in Fig. 1.[1] Both the legitimate and illegitimate receivers are equipped with a single antenna. It is assumed that the fading coefficients between each antenna at S and destinations

[1] Although only two users were considered in this works, the results can be easily extended to the downlink NOMA system with N ($N > 2$) users. For example, the hybrid multiple access scheme proposed in [13] and [14], where NOMA scheme is implemented among the users within each group, while the conventional OMA scheme is utilized for inter-group multiple access. In these scenarios, in order to decrease the complexity of message detection, a user pairing technique can be used to ensure that only two users share a specific orthogonal resource slot [28].

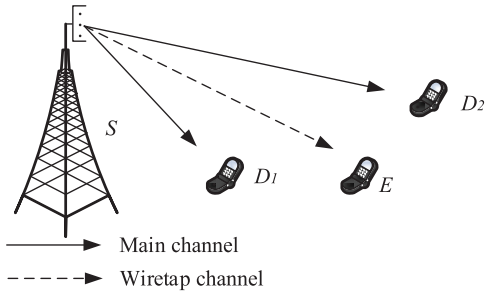

FIGURE 1. System model consisting of a transmitting source (S) equipped with multiple antennas, two legitimate receivers (D_1 and D_2), and an illegitimate eavesdropper (E).

(including D_1, D_2, and E) experience independent Rayleigh fading.

Under NOMA scheme, the signal received at D_m can be expressed as

$$y_{D_m} = h_{D_m}\left(\sqrt{a_1 P_S}x_1 + \sqrt{a_2 P_S}x_2\right) + n_m, \tag{1}$$

where $m = \{1, 2\}$, h_{D_m} denotes the channel coefficient between S and D_m, a_m represents the power allocation coefficients, $a_1 + a_2 = 1$, P_S denotes the transmit power at S, and x_m represents the messages to D_m. n_m is complex additive white Gaussian noise (AWGN) with zero mean and variance σ_m^2, For simplicity, we assume $\sigma_1^2 = \sigma_2^2 = \sigma^2$.

In this work, it is assumed that users are not ordered by their channel conditions.[2] Under NOMA scheme [6], D_1 can detect x_1 by using SIC and x_1 will be regarded as interference when D_2 decodes its received signal. Therefore, the received instantaneous signal-to-interference-noise ratio (SINR) of the m-th user can be given as [6]

$$\gamma_{D_m} = \begin{cases} a_1\rho\left|h_{D_1}\right|^2, & m = 1 \\ \dfrac{\left|h_{D_2}\right|^2 a_2}{\left|h_{D_2}\right|^2 a_1 + \frac{1}{\rho}}, & m = 2, \end{cases} \tag{2}$$

where $\rho = P_S/\sigma^2$ sigifies the transmit SNR where P_S is the transmit power at the S.

In [27] and [28], the authors assumed that the eavesdropper has enough powerful capabilities to detect multiuser data and extracts the signal to D_m when it eavesdrops D_m. It is a pessimistic assumption since the multi-user decoding ability of E is overestimated.

In this work, we assume E can eliminate the signal to D_2 by SIC when it eavesdrops D_1 and treats the message to D_1 as noise when it eavesdrops D_2.[3]

[2]In these scenarios, users are categorized by their quality of service requirements. Similar assumptions can be found in [32], and [33], in which user 1 was assumed to be served opportunistically and user 2 was assumed to be served for small packet transmission.

[3]For the wiretap scenarios with multiple users, it is assumed that the $m-1$ users' messages have already been decoded before the eavesdropper tries to decode the mth user's message. Similar assumptions can be found in [26]. Obviously, this assumption overestimates the eavesdropper's capability and is pessimistic, then our results will be a lower bound of practical cases.

Thus, we have

$$\gamma_{E_m} = \begin{cases} a_1\rho|h_E|^2, & m = 1 \\ \dfrac{a_2|h_E|^2}{a_1|h_E|^2 + \frac{1}{\rho}}, & m = 2, \end{cases} \tag{3}$$

where h_E is the channel coefficient and γ_{E_m} is the SINR when it eavesdrops the transmitted signal to receiver D_m $(m = 1, 2)$, respectively. The cumulative distribution function (CDF) of γ_{k_m} $(k \in \{D, E\}, m = 1, 2)$ can be written as

$$F_{\gamma_{k_1}}(\gamma) = 1 - e^{-\frac{\gamma}{\lambda_{k_1} a_1 \rho}}, \tag{4}$$

$$F_{\gamma_{k_2}}(\gamma) = \begin{cases} 1 - \varphi\left(\lambda_{k_2}, \gamma\right), & \gamma < \dfrac{a_2}{a_1} \\ 1, & \gamma \geq \dfrac{a_2}{a_1}, \end{cases} \tag{5}$$

respectively, where $\varphi(\xi, x) = e^{-\frac{x}{\xi\rho(a_2 - a_1 x)}}$, λ_{k_m} represents the average channel power gain. In this work, it is assumed that $\lambda_{E_1} = \lambda_{E_2} = \lambda_E$ for simplification.

The probability density function (PDF) of γ_{k_m} $(k \in \{D, E\}, m = 1, 2)$ can be obtained as

$$f_{\gamma_{k_1}}(\gamma) = \frac{1}{\lambda_{k_1} a_1 \rho} e^{-\frac{\gamma}{\lambda_{k_1} a_1 \rho}}, \tag{6}$$

$$f_{\gamma_{k_2}}(\gamma) = \begin{cases} \dfrac{a_2}{\lambda_{k_2}\rho(a_2 - a_1\gamma)^2}\varphi\left(\lambda_{k_2}, \gamma\right), & \gamma < \dfrac{a_2}{a_1} \\ 0, & \gamma \geq \dfrac{a_2}{a_1}. \end{cases} \tag{7}$$

III. SECRECY OUTAGE PROBABILITY ANALYSIS OF A SISO NOMA SYSTEM

In this section, we consider a two-user NOMA system with a single-antenna base station, as motivated by the following reasons: 1) preparing for the performance analysis of MISO NOMA systems; 2) setting up a benchmark for comparing the performance of MISO NOMA systems to testify the enhancement befitted from using the multiple antennas at S.

The instantaneous secrecy capacity of D_m $(m = 1, 2)$ can be expressed as [25]

$$C_{s,m} = \left[\log_2\left(1 + \gamma_{D_m}\right) - \log_2\left(1 + \gamma_{E_m}\right)\right]^+, \tag{8}$$

where $[x]^+ = \max\{x, 0\}$.

SOP is defined as the probability that the secrecy capacity is less than a preset target rate. Thus, the SOP at D_m $(m = 1, 2)$ can be expressed as

$$\begin{aligned} P_{out,D_m} &= \Pr\left\{C_{s,m} \leq R_{s,m}\right\} \\ &= \int_0^\infty F_{\gamma_{D_m}}\left(\Theta_m\gamma + \Theta_m - 1\right) f_{\gamma_{E_m}}(\gamma)\, d\gamma, \end{aligned} \tag{9}$$

where $R_{s,m}$ denotes the target rate at D_m and $\Theta_m = 2^{R_{s,m}} \geq 1$.

Substituting (4) and (6) into (9), and using [34, eq. (3.381.4)], the SOP at D_1 can be expressed as

$$P_{out,D_1} = 1 - \frac{\lambda_{D_1}}{\Theta_1\lambda_E + \lambda_{D_1}} e^{-\frac{\Theta_1 - 1}{a_1\rho\lambda_{D_1}}}. \tag{10}$$

Observing (10), one can deduce that the SOP at D_1 will be improved when the transmit SNR (ρ) increases. Furthermore, there exists a floor at $\frac{\Theta_1\lambda_E}{\Theta_1\lambda_E+\lambda_{D_1}}$ for P_{out,D_1} as $\rho \to \infty$ since the average secrecy capacity will reach a ceiling, which is testified in [35].

Lemma 1: the SOP at D_2 is expressed as

$$P_{out,D_2} = 1 - \frac{a_2\varpi\pi}{2N\lambda_E\rho}\sum_{n=1}^{N}\frac{\sqrt{1-\tau_n{}^2}}{(a_2-a_1\vartheta_n)^2}e^{-B_n}, \quad (11)$$

where $B_n = \frac{\Theta_2(1+\vartheta_n)-1}{\lambda_{D_2}\rho(a_2-a_1(\Theta_2(1+\vartheta_n)-1))} + \frac{\vartheta_n}{\lambda_E\rho(a_2-a_1\vartheta_n)}$, N is the number of terms, $\tau_n = \cos\left(\frac{2n-1}{2N}\pi\right)$ and $\vartheta_n = \frac{\varpi(\tau_n+1)}{2}$.

Proof: Substituting (5) and (7) into (9), we obtain

$$\begin{aligned} &P_{out,D_2} \\ &= \int_0^{\varpi} F_{\gamma_{D_2}}(\Theta_2\gamma+\Theta_2-1)f_{\gamma_{E_2}}(\gamma)d\gamma + \int_{\varpi}^{\frac{a_2}{a_1}} f_{\gamma_{E_2}}(\gamma)d\gamma \\ &= 1 - \underbrace{\int_0^{\varpi}\varphi\left(\lambda_{D_2},\Theta_2\gamma+\Theta_2-1\right)f_{\gamma_{E_2}}(\gamma)d\gamma}_{\triangleq\chi}, \end{aligned} \quad (12)$$

where $\varpi = \frac{1}{a_1\Theta_2} - 1 \le \frac{a_2}{a_1}$. To the best of the authors' knowledge, it is very difficult to obtain the closed-form expression of χ. Using Gaussian-Chebyshev quadrature [36, eq. (25.4.38)], χ is approximated as

$$\begin{aligned} \chi &= \frac{a_2}{\lambda_E\rho}\int_0^{\varpi}\frac{1}{(a_2-a_1\gamma)^2} \\ &\quad\times e^{-\left(\frac{\Theta_2\gamma+\Theta_2-1}{\lambda_{D_2}\rho(a_2-a_1(\Theta_2-1)-a_1\Theta_2\gamma)}+\frac{\gamma}{\lambda_E\rho(a_2-a_1\gamma)}\right)}d\gamma \\ &= \frac{a_2\varpi\pi}{2N\lambda_E\rho}\sum_{n=1}^{N}\frac{\sqrt{1-\tau_n{}^2}}{(a_2-a_1\vartheta_n)^2}e^{-B_n}. \end{aligned} \quad (13)$$

Remark 1: We rewrite P_{out,D_2} as

$$P_{out,D_2} = 1 - \sum_{n=1}^{N}\frac{A_n}{\rho}e^{-\frac{B_n}{\rho}}, \quad (14)$$

where $A_n = \frac{a_2\varpi\pi}{2N\lambda_E}\frac{\sqrt{1-\tau_n{}^2}}{(a_2-a_1\vartheta_n)^2} > 0$, $B_n > 0$.

We obtain

$$\frac{d\left(P_{out,D_2}\right)}{d\rho} = \sum_{n=1}^{N}\frac{A_n}{\rho^2}e^{-\frac{B_n}{\rho}}\left(1-\frac{B_n}{\rho}\right). \quad (15)$$

One can find that $\frac{d\left(P_{out,D_2}\right)}{d\rho}$ is negative within a certain range (ρ is lower), else $\frac{d\left(P_{out,D_2}\right)}{d\rho}$ is positive. That is to say that P_{out,D_2} will decrease within a certain range as ρ increases, else it will increase in the other ranges. There is an optimal ρ that can obtain the best SOP. This is the main difference between P_{out,D_1} and P_{out,D_2}. That means increasing the transmit power may degrade the SOP of two-user NOMA system.

It is assumed that E is interested only in a specific user's message, but the transmitter does not know which user E wants to wiretap. Hence the SOP for the two-user NOMA system can be expressed as[4]

$$\begin{aligned} P_{out} &= \Pr\{D_1 \text{ secrecy outage or } D_2 \text{ secrecy outage}\} \\ &= \Pr\{D_1 \text{ secrecy outage, } E \text{ eavesdrops } D_1\} \\ &\quad + \Pr\{D_2 \text{ secrecy outage, } E \text{ eavesdrops } D_2\} \\ &= \Pr\{D_1 \text{ secrecy outage} \,|\text{when } E \text{ eavesdrops } D_1\} \\ &\quad\times \Pr\{E \text{ eavesdrops } D_1\} \\ &\quad + \Pr\{D_2 \text{ secrecy outage} \,|\text{when } E \text{ eavesdrops } D_2\} \\ &\quad\times \Pr\{E \text{ eavesdrops } D_2\} \\ &= P_{out,D_1}\times\Pr\{E \text{ eavesdrops } D_1\} \\ &\quad + P_{out,D_2}\times\Pr\{E \text{ eavesdrops } D_2\}. \end{aligned} \quad (16)$$

$\Pr\{E \text{ eavesdrop } D_1\}$ and $\Pr\{E \text{ eavesdrop } D_2\}$ can be analyzed based on practical scenarios. To simplify the analysis, it is assumed that $\Pr\{E \text{ eavesdrop } D_1\} = \Pr\{E \text{ eavesdrop } D_1\} = \frac{1}{2}$. Then the SOP for the two-user NOMA system is expressed as

$$P_{out} = \frac{1}{2}\left(P_{out,D_1} + P_{out,D_2}\right). \quad (17)$$

IV. SECRECY OUTAGE PROBABILITY ANALYSIS OF A MISO NOMA SYSTEMS

In this section, the secrecy outage performance of a MISO NOMA system with different TAS schemes utilized at S is analyzed. Firstly, we analyze the secrecy outage performance with OAS and SAS schemes, depending on whether the global CSI is available at the base station. To better demonstrate the enhancement of TAS schemes, we consider the STT scheme as a benchmark, wherein all the antennas are utilized to send the message with equal power.

A. THE OPTIMAL ANTENNA SELECTION SCHEME

In those scenarios where the users play dual roles as legitimate receivers for some signals and eavesdroppers for others, the eavesdropper is active (e.g., in a time-division multiple-access (TDMA) environment) such that the source node can estimate the eavesdropper's channel during the eavesdropper's transmissions [37], [38]. When the CSI of both the wiretap and main links are known at the base station, the antenna that maximizes the secrecy capacity is optimal [29], [30]. In this subsection we will analyze the SOP of MISO NOMA systems while considering D_1 or D_2, respectively.

Firstly, we consider the case that the secrecy issue of D_1 is more important than the one of D_2, the transmit antenna is selected based on the secrecy capacity performance of D_1. The instantaneous secrecy capacity for such scenarios can be expressed as [30]

$$C_{s,1}^{\text{OAS}} = \max_{i\in N_S}\left\{C_{s,1}^{i\text{OAS}}\right\}, \quad (18)$$

[4] In [27] and [28], a different definition of the SOP for the selected user pair was given as $P_{out} = 1-\left(1-P_{out,D_1}\right)\left(1-P_{out,D_1}\right)$. The results with this definition can be easily obtained with the results of our work and the same conclusion can be observed. Here we assume that E can not eavesdrop both the users simultaneously.

where $C_{s,1}^{i\text{OAS}} = \left[\log_2\left(1+\gamma_{D_1}^{i\text{OAS}}\right) - \log_2\left(1+\gamma_{E_1}^{i\text{OAS}}\right)\right]^+$ is the instantaneous secrecy capacity of D_1 when S is equipped with a single antenna.

The SOP at D_1 in the MISO NOMA system can be expressed as

$$P_{out,D_1}^{\text{OAS}} = \Pr\left\{\max_{i\in N_S}\left\{C_{s,1}^{i\text{OAS}}\right\} \le R_{s,1}\right\} = \prod_{i=1}^{N_S}\Pr\left\{C_{s,1}^{i\text{OAS}} \le R_{s,1}\right\} = \left(P_{out,D_1}^{i\text{OAS}}\right)^{N_S}, \quad (19)$$

where $P_{out,D_1}^{i\text{OAS}} = \Pr\left\{C_{s,1}^{i\text{OAS}} \le R_{s,1}\right\}$ is the SOP at D_1 when S is equipped with a single antenna. Obviously, we have $P_{out,D_1}^{i\text{OAS}} = P_{out,D_1}$.

It is noted that selecting the optimal transmit antenna for D_1 corresponds to selecting a random transmit antenna for D_2, which means the SOP at D_2 in this scenario can also be given by (12).

When the transmitting antenna is selected based on D_1, the overall SOP can be expressed as

$$P_{out}^{\text{OAS},1} = \frac{1}{2}\left(\left(P_{out,D_1}\right)^{N_S} + P_{out,D_2}\right). \quad (20)$$

Similarly, we obtain the SOP with OAS scheme based on D_2 as

$$P_{out}^{\text{OAS},2} = \frac{1}{2}\left(P_{out,D_1} + \left(P_{out,D_2}\right)^{N_S}\right). \quad (21)$$

B. THE SUBOPTIMAL ANTENNA SELECTION SCHEME

When the CSI of the wiretap link is not available at the base station, the best transmit antenna is selected to maximize the capacity of the main channel [29], [30].[5] We analyze the secrecy outage performance for MISO NOMA systems while considering D_1 or D_2, respectively.

1) SAS SCHEME CONSIDERING D_1

When D_1 is more important than D_2 for some practical reasons, the transmit antenna is selected based on the capacity of $S-D_1$ link, which means $\gamma_{D_1}^{\text{SAS},1} = \max_{1\le i\le N_S}\left\{\gamma_{S_iD_1}\right\}$, where $\gamma_{S_iD_1}$ means the received instantaneous SINR at the near user from the i-th antenna at S. The CDF and PDF of $\gamma_{S_iD_1}$ are the same as (4) and (6). Then the CDF of $\gamma_{D_1}^{\text{SAS},1}$ can be obtained as

$$F_{\gamma_{D_1}}^{\text{SAS}}(\gamma) = \left(F_{\gamma_{D_1}}(\gamma)\right)^{N_S} = \sum_{i=0}^{N_S}\frac{(-1)^i N_S!}{i!\,(N_S-i)!}e^{-\frac{i\gamma}{\lambda_{D_1}a_1\rho}}. \quad (22)$$

Note that selecting the optimal transmit antenna for D_1 corresponds to selecting a random transmit antenna for D_2 and E, which means the CDF and PDF of $\gamma_{D_2}^{\text{SAS},1}$ and $\gamma_{E_m}^{\text{SAS},1}$ are same as (5) and (7), respectively. Thus the SOP at D_2 in this case is given by (12).

Substituting (7) and (22) into (9) and making use of [34, eq. (3.351.3)], we obtain

$$P_{out,D_1}^{\text{SAS}} = \int_0^\infty F_{\gamma_{D_1}}^{\text{SAS}}\left(\Theta_1(1+\gamma)-1\right)f_{\gamma_{E_2}}(\gamma)\,d\gamma = \sum_{i=0}^{N_S}\frac{(-1)^i N_S!\lambda_{D_1}}{i!\,(N_S-i)!\left(i\Theta_1\lambda_E+\lambda_{D_1}\right)}e^{-\frac{i(\Theta_1-1)}{a_1\rho\lambda_{D_1}}}. \quad (23)$$

The SOP that maximizes the capacity of $S-D_1$ link is obtained by substituting (12) and (23) into (17) as

$$P_{out}^{\text{SAS},1} = \frac{1}{2}\left(P_{out,D_1}^{\text{SAS}} + P_{out,D_2}\right). \quad (24)$$

2) SAS SCHEME CONSIDERING D_2

Similarly, when transmit antenna is selected based on the capacity of $S-D_2$ link, the CDF and PDF of $\gamma_{D_1}^{\text{SAS},2}$ and $\gamma_{E_m}^{\text{SAS},2}$ are same as (5) and (7), respectively. The SOP at D_1 in this case is given by (10).

The CDF of $\gamma_{D_2}^{\text{SAS},2}$ is obtained as

$$F_{\gamma_{D_2}}^{\text{SAS}}(\gamma) = \begin{cases}\displaystyle\sum_{i=0}^{N_S}\frac{(-1)^i N_S!}{i!\,(N_S-i)!}e^{-\frac{i\gamma}{\lambda_{D_2}\rho(a_2-a_1\gamma)}}, & \gamma < \dfrac{a_2}{a_1}\\ 1, & \gamma \ge \dfrac{a_2}{a_1}.\end{cases} \quad (25)$$

Lemma 2: The SOP at D_2 in the case with SAS scheme considering D_2 is expressed as

$$P_{out,D_2}^{\text{SAS}} = \frac{\varpi\pi a_2 N_S!}{2\rho N\lambda_E}\sum_{i=0}^{N_S}\sum_{n=1}^{N}\frac{(-1)^i\sqrt{1-\tau_n^2}e^{-\Phi}}{i!\,(N_S-i)!(a_2-a_1\vartheta_n)^2} + e^{-\frac{\varpi}{\lambda_E\rho(a_2-a_1\varpi)}}, \quad (26)$$

where $\Phi = \frac{i(\Theta_2(1+\vartheta_n)-1)}{\lambda_{D_2}\rho(a_2-a_1(\Theta_2(1+\vartheta_n)-1))} + \frac{\vartheta_n}{\lambda_E\rho(a_2-a_1\vartheta_n)}$.

Proof: Substituting (7) and (25) into (9), we obtain

$$P_{out,D_2}^{\text{SAS}} = \underbrace{\int_0^\varpi F_{\gamma_{D_2}}^{\text{SAS}}\left(\Theta_2(1+\gamma)-1\right)f_{\gamma_{E_2}}(\gamma)\,d\gamma}_{I_1^{\text{SAS},2}} + \underbrace{\int_\varpi^{\frac{a_2}{a_1}} f_{\gamma_{E_2}}(\gamma)\,d\gamma}_{I_2^{\text{SAS},2}}. \quad (27)$$

Using (7), (25) and Gaussian-Chebyshev quadrature method, we can achieve

$$I_1^{\text{SAS},2} = \sum_{i=0}^{N_S}\frac{(-1)^i a_2 N_S!}{i!\,(N_S-i)!\lambda_E\rho}\int_0^\varpi \frac{1}{(a_2-a_1\gamma)^2} \times e^{-\frac{i(\Theta_2(1+\gamma)-1)}{\lambda_{D_2}\rho(a_2-a_1(\Theta_2(1+\gamma)-1))}-\frac{\gamma}{\lambda_E\rho(a_2-a_1\gamma)}}d\gamma = \frac{\varpi\pi a_2 N_S!}{2\rho N\lambda_E}\sum_{i=0}^{N_S}\sum_{n=1}^{N}\frac{(-1)^i\sqrt{1-\tau_n^2}e^{-\Phi}}{i!\,(N_S-i)!(a_2-a_1\vartheta_n)^2}. \quad (28)$$

[5] Note that selecting the strongest transmit antenna for the destination node corresponds to selecting a random transmit antenna for E. Thus the secrecy capacity with this scheme may not be the maximum and then this scheme is called suboptimal antenna selection scheme.

Using (7), we can easily obtain

$$I_2^{\mathrm{SAS},2} = e^{-\frac{\varpi}{\lambda_E \rho (a_2 - a_1 \varpi)}}. \tag{29}$$

The SOP in this case is obtained by substituting (10) and (26) into (17) as

$$P_{out}^{\mathrm{SAS},2} = \frac{1}{2}\left(P_{out,D_1} + P_{out,D_2}^{\mathrm{SAS}}\right). \tag{30}$$

C. THE SPACE-TIME TRANSMISSION SCHEME

To demonstrate the enhancement of TAS scheme, in this subsection we analyze the SOP with the traditional STT scheme wherein all the antennas are utilized to transmit signals with power $\frac{P_S}{N_S}$ [29], [30]. It is assumed that the selection combination (SC) scheme is utilized at both legitimate and illegitimate receivers, which means $\gamma_{k_m}^{\mathrm{STT}} = \max_{1 \le i \le N_S} \{\gamma_{S_i k_m}\}$. With some simple algebraic manipulations, the CDF and PDF of γ_{k_m} ($k \in \{D, E\}$, $m = 1, 2$) can be expressed as

$$F_{\gamma_{k_1}}^{\mathrm{STT}}(\gamma) = \sum_{i=0}^{N_S} \frac{(-1)^i N_S!}{i!\,(N_S - i)!} e^{-\frac{iN_S\gamma}{\lambda_{k_1} a_1 \rho}}, \tag{31}$$

$$F_{\gamma_{k_2}}^{\mathrm{STT}}(\gamma) = \begin{cases} \sum_{i=0}^{N_S} \frac{(-1)^i N_S!}{i!\,(N_S - i)!} e^{-\frac{iN_S\gamma}{\lambda_{k_2}\rho(a_2 - a_1\gamma)}}, & \gamma < \frac{a_2}{a_1} \\ 1, & \gamma \ge \frac{a_2}{a_1}, \end{cases} \tag{32}$$

$$f_{\gamma_{k_1}}^{\mathrm{STT}}(\gamma) = \frac{{N_S}^2}{\lambda_{k_1} a_1 \rho} \sum_{i=0}^{N_S - 1} \frac{(-1)^i (N_S - 1)!}{i!\,(N_S - 1 - i)!} e^{-\frac{(i+1)N_S\gamma}{\lambda_{k_1} a_1 \rho}}, \tag{33}$$

$$f_{\gamma_{k_2}}^{\mathrm{STT}}(\gamma) = \begin{cases} \frac{a_2 {N_S}^2}{\lambda_{k_2}\rho(a_2 - a_1\gamma)^2} \sum_{i=0}^{N_S-1} \frac{(-1)^i}{i!} \\ \quad \times \frac{(N_S - 1)!}{(N_S - 1 - i)!} e^{-\frac{(i+1)N_S\gamma}{\lambda_{k_2}\rho(a_2 - a_1\gamma)}}, & \gamma < \frac{a_2}{a_1} \\ 0, \quad \gamma \ge \frac{a_2}{a_1}, \end{cases} \tag{34}$$

respectively.

Substituting (31) and (33) into (9) and making use of [34, eq. (3.351.3)], we obtain

$$\begin{aligned} P_{out,D_1}^{\mathrm{STT}} &= \int_0^{\infty} F_{\gamma_{D_1}}^{\mathrm{STT}}(\Theta_1\gamma + \Theta_1 - 1) f_{\gamma_{E_1}}^{\mathrm{STT}}(\gamma)\, d\gamma \\ &= \frac{{N_S}^2}{\lambda_E a_1 \rho} \sum_{i=0}^{N_S} \sum_{j=0}^{N_S - 1} \frac{(-1)^{i+j} N_S!}{i!\,(N_S - i)!} \frac{(N_S - 1)!}{j!\,(N_S - 1 - j)!} \\ &\quad \times e^{-\frac{iN_S(\Theta_1 - 1)}{\lambda_{D_1} a_1 \rho}} \int_0^{\infty} e^{-\frac{\left(i\Theta_1\lambda_E + (j+1)\lambda_{D_1}\right)N_S\gamma}{\lambda_{D_1}\lambda_E a_1 \rho}} d\gamma \\ &= \sum_{i=0}^{N_S} \sum_{j=0}^{N_S - 1} \frac{(-1)^{i+j} N_S!}{i!\,(N_S - i)!} \frac{(N_S - 1)!}{j!\,(N_S - 1 - j)!} \\ &\quad \times \frac{N_S \lambda_{D_1}}{i\Theta_1\lambda_E + \lambda_{D_1}(j+1)} e^{-\frac{iN_S(\Theta_1 - 1)}{\lambda_{D_1} a_1 \rho}}. \end{aligned} \tag{35}$$

Lemma 3: The SOP at D_2 in the case with STT scheme is expressed as

$$\begin{aligned} P_{out,D_2}^{\mathrm{STT}} &= \frac{a_2 \varpi \pi {N_S}^2}{2\rho N \lambda_E} \sum_{i=0}^{N_S} \sum_{j=0}^{N_S - 1} \sum_{n=1}^{N} \frac{\psi \sqrt{1 - \tau_n^2}\, e^{-\Psi}}{(a_2 - a_1\vartheta_n)^2} \\ &\quad + 1 - \sum_{i=0}^{N_S} \frac{(-1)^i N_S!}{i!\,(N_S - i)!} e^{-\frac{i\varpi N_S}{\lambda_E \rho (a_2 - a_1 \varpi)}}, \end{aligned} \tag{36}$$

where

$$\psi = \frac{(-1)^{j+i} N_S!}{i!\,(N_S - i)!} \frac{(N_S - 1)!}{j!\,(N_S - 1 - j)!}$$

and

$$\Psi = \frac{iN_S\left(\Theta_2\vartheta_n + \Theta_2 - 1\right)}{\lambda_{D_2}\rho\left(a_2 - a_1\left(\Theta_2\vartheta_n + \Theta_2 - 1\right)\right)} + \frac{(j+1)N_S\vartheta_n}{\lambda_E \rho\left(a_2 - a_1\vartheta_n\right)}.$$

Proof: Substituting (32) and (34) into (9), we obtain

$$\begin{aligned} P_{out,D_2}^{\mathrm{STT}} &= \underbrace{\int_0^{\varpi} F_{\gamma_{D_2}}^{\mathrm{STT}}(\Theta_2\gamma + \Theta_2 - 1) f_{\gamma_{E_2}}^{\mathrm{STT}}(\gamma)\, d\gamma}_{I_1^{\mathrm{STT}}} \\ &\quad + \underbrace{\int_{\varpi}^{\frac{a_2}{a_1}} f_{\gamma_{E_2}}^{\mathrm{STT}}(\gamma) d\gamma}_{I_2^{\mathrm{STT}}}. \end{aligned} \tag{37}$$

Utilizing (32), (34), and Gaussian-Chebyshev quadrature method, we obtain

$$\begin{aligned} I_1^{\mathrm{STT}} &= \frac{a_2 {N_S}^2}{\rho\lambda_E} \sum_{i=0}^{N_S} \sum_{j=0}^{N_S - 1} \psi \int_0^{\varpi} \frac{1}{(a_2 - a_1\gamma)^2} \\ &\quad \times e^{-\frac{iN_S(\Theta_2\gamma + \Theta_2 - 1)}{\lambda_{D_2}\rho(a_2 - a_1(\Theta_2\gamma + \Theta_2 - 1))} - \frac{(j+1)N_S\gamma}{\lambda_E\rho(a_2 - a_1\gamma)}} d\gamma \\ &= \frac{a_2 \varpi \pi {N_S}^2}{2\rho N \lambda_E} \sum_{i=0}^{N_S} \sum_{j=0}^{N_S - 1} \sum_{n=1}^{N} \frac{\psi \sqrt{1 - \tau_n^2}\, e^{-\Psi}}{(a_2 - a_1\vartheta_n)^2}. \end{aligned} \tag{38}$$

Using (32), we obtain

$$I_2^{\mathrm{STT}} = 1 - \sum_{i=0}^{N_S} \frac{(-1)^i N_S!}{i!\,(N_S - i)!} e^{-\frac{i\varpi N_S}{\lambda_E \rho (a_2 - a_1 \varpi)}}. \tag{39}$$

Finally, substituting (35) and (36) into (17), the SOP of MISO NOMA system with STT scheme is obtained as

$$P_{out}^{\mathrm{STT}} = \frac{1}{2}\left(P_{out,D_1}^{\mathrm{STT}} + P_{out,D_2}^{\mathrm{STT}}\right). \tag{40}$$

V. ASYMPTOTIC SECRECY OUTAGE PROBABILITY ANALYSIS

In order to get more insights, we analyze the secrecy outage performance in the high SINR regime, which is mathematically described as $\lambda_{D_2} \to \infty$ and $\lambda_{D_1} = \beta\lambda_{D_2}$ ($\beta > 1$). The secrecy diversity order is expressed as [30]

$$G_{d,m} = -\lim_{\lambda_{D_2} \to \infty} \frac{\ln P_{out,D_m}^{\infty}}{\ln \lambda_{D_2}}, \tag{41}$$

where P_{out,D_m}^{∞} denotes the asymptotic SOP.

A. SISO NOMA SYSTEMS

Using (4), (5), and $e^x = \sum_{m=0}^{k} \frac{x^m}{m!} + \mathcal{O}\left(x^k\right)$, we obtain $F^{\infty}_{\gamma_{D_1}}(\gamma)$ and $F^{\infty}_{\gamma_{D_2}}(\gamma)$ as

$$F^{\infty}_{\gamma_{D_1}}(\gamma) = \frac{\gamma}{\beta\lambda_{D_2}a_1\rho}, \tag{42}$$

$$F^{\infty}_{\gamma_{D_2}}(\gamma) = \begin{cases} \dfrac{\gamma}{\lambda_{D_2}\rho\left(a_2 - a_1\gamma\right)} & \gamma < \dfrac{a_2}{a_1} \\ 1, & \gamma \geq \dfrac{a_2}{a_1}, \end{cases} \tag{43}$$

respectively.

Substituting (6) and (42) into (9) and making use of (3.381.4) of [34], we obtain the asymptotic SOP at D_1 as

$$\begin{aligned} P^{\infty}_{out,D_1} &= \int_0^{\infty} F^{\infty}_{\gamma_{D_1}}\left(\Theta_1\left(1+\gamma\right)-1\right) f_{\gamma_{E_1}}(\gamma)\, d\gamma \\ &= \frac{\Theta_1 - 1 + \Theta_1\lambda_E a_1\rho}{\beta\lambda_{D_2}a_1\rho}. \end{aligned} \tag{44}$$

Similarly, making use of Gaussian-Chebyshev quadrature method, the asymptotic SOP at D_2 is obtained as

$$\begin{aligned} P^{\infty}_{out,D_2} &= \int_0^{\varpi} F^{\infty}_{\gamma_{D_2}}\left(\Theta_2\gamma + \Theta_2 - 1\right) f_{\gamma_{E_2}}(\gamma)\, d\gamma \\ &\quad + \int_{\varpi}^{\frac{a_2}{a_1}} f_{\gamma_{E_2}}(\gamma)\, d\gamma \\ &= e^{-\frac{\varpi}{\lambda_E\rho\left(a_2 - a_1\varpi\right)}} + \frac{a_2}{\lambda_{D_2}\lambda_E\rho^2} \\ &\quad \times \int_0^{\varpi} \frac{\left(\Theta_2\gamma + \Theta_2 - 1\right) e^{-\frac{\gamma}{\lambda_E\rho\left(a_2 - a_1\gamma\right)}}\, d\gamma}{\left(a_2 - a_1\left(\Theta_2\left(1+\gamma\right)-1\right)\right)\left(a_2 - a_1\gamma\right)^2} \\ &= e^{-\frac{\varpi}{\lambda_E\rho\left(a_2 - a_1\varpi\right)}} + \frac{a_2\varpi\pi}{2N\lambda_{D_2}\lambda_E\rho^2} \\ &\quad \times \sum_{n=1}^{N} \frac{\left(\Theta_2(1+\vartheta_n)-1\right)\sqrt{1-\tau_n{}^2}\, e^{-\frac{\vartheta_n}{\lambda_E\rho\left(a_2 - a_1\vartheta_n\right)}}}{\left(a_2 - a_1\left(\Theta_2(1+\vartheta_n)-1\right)\right)\left(a_2 - a_1\vartheta_n\right)^2}. \end{aligned} \tag{45}$$

Remark 2: Based on (44) and (45), one can easily obtain the secrecy diversity order of the near and far users as 1 and 0, respectively. This is because P^{∞}_{out,D_2} will become a constant when $\lambda_{D_2} \to \infty$. Furthermore, this means that increasing the transmit power does not have any impact on the secrecy performance of D_2.

Finally, the overall SOP is obtained by substituting (44) and (45) into (17). The secrecy diversity order of SISO NOMA system is easily obtained as $G_d^{\text{SISO}} = 0$ since the secrecy diversity order of two-user NOMA is determined by the one that has small diversity order [28].

B. MISO NOMA SYSTEMS WITH SAS SCHEME

When $\lambda_{D_2} \to \infty$ and $\lambda_{D_1} = \beta\lambda_{D_2}$, we have

$$F^{\infty,\text{SAS}}_{\gamma_{D_1}}(\gamma) = \frac{\gamma^{N_S}}{\left(\beta\lambda_{D_2}a_1\rho\right)^{N_S}}, \tag{46}$$

$$F^{\infty,\text{SAS}}_{\gamma_{D_2}}(\gamma) = \begin{cases} \dfrac{\gamma^{N_S}}{\left(\lambda_{D_2}\rho\left(a_2 - a_1\gamma\right)\right)^{N_S}} & \gamma < \dfrac{a_2}{a_1} \\ 1, & \gamma \geq \dfrac{a_2}{a_1}. \end{cases} \tag{47}$$

By substituting (6) and (46) into (9) and using of [34, eq. (3.351.3)], we obtain

$$\begin{aligned} P^{\infty,\text{SAS}}_{out,D_1} &= \int_0^{\infty} F^{\infty,\text{SAS}}_{\gamma_{D_1}}\left(\Theta_1\left(1+\gamma\right)-1\right) f_{\gamma_{E_1}}(\gamma)\, d\gamma \\ &= \frac{N_S!}{\lambda_E\left(\beta\lambda_{D_2}\right)^{N_S}\left(a_1\rho\right)^{N_S+1}} \\ &\quad \times \sum_{k=0}^{N_S} \frac{\Theta_1^k(\Theta_1-1)^{N_S-k}}{k!\left(N_S-k\right)!} \int_0^{\infty} \gamma^k e^{-\frac{\gamma}{\lambda_E a_1\rho}}\, d\gamma \\ &= \frac{N_S!}{\beta^{N_S}{\lambda_{D_2}}^{N_S}} \sum_{k=0}^{N_S} \frac{\Theta_1^k(\Theta_1-1)^{N_S-k}{\lambda_E}^k}{(N_S-k)!(a_1\rho)^{N_S-k}}. \end{aligned} \tag{48}$$

Substituting (7) and (47) into (27) and utilizing Gaussian-Chebyshev quadrature method, we obtain

$$\begin{aligned} P^{\infty,\text{SAS}}_{out,D_2} &= \int_0^{\infty} F^{\infty,\text{SAS}}_{\gamma_{D_2}}\left(\Theta_2\left(1+\gamma\right)-1\right) f_{\gamma_{E_2}}(\gamma)\, d\gamma \\ &= I_2^{\text{SAS},2} + \int_0^{\varpi} \frac{a_2 e^{-\frac{\gamma}{\lambda_E\rho\left(a_2 - a_1\gamma\right)}}}{\lambda_E\rho\left(a_2 - a_1\gamma\right)^2} \\ &\quad \times \frac{\left(\Theta_2\left(1+\gamma\right)-1\right)^{N_S} d\gamma}{\left(\lambda_{D_2}\rho\left(a_2 - a_1\left(\Theta_2\left(1+\gamma\right)-1\right)\right)\right)^{N_S}} \\ &= I_2^{\text{SAS},2} + \Xi_1 \sum_{n=1}^{N} e^{-\frac{\vartheta_n}{\lambda_E\rho\left(a_2 - a_1\vartheta_n\right)}} \\ &\quad \times \frac{\sqrt{1-\tau_n{}^2}\left(\Theta_2\left(1+\vartheta_n\right)-1\right)^{N_S}}{\left(1 - a_1\Theta_2\left(1+\vartheta_n\right)\right)^{N_S}\left(a_2 - a_1\vartheta_n\right)^2}, \end{aligned} \tag{49}$$

where $\Xi_1 = \frac{\varpi\pi a_2}{2N\lambda_E\rho^{N_S+1}{\lambda_{D_2}}^{N_S}}$.

Substituting (48) and (49) into (24) and (30), respectively, the asymptotic SOP for MISO NOMA system with SAS scheme is obtained. The secrecy diversity order for SAS scheme while considering D_1 or D_2 is N_S and 0, respectively. One can easily obtain the diversity order of two-user MISO NOMA system for SAS scheme considering D_1 and D_2 as

$$G_d^{\text{SAS},1} = G_d^{\text{SAS},2} = 0. \tag{50}$$

C. MISO NOMA SYSTEMS WITH OAS SCHEME

Substituting (44) and (45) into (20) and (21), respectively, the asymptotic SOP for MISO NOMA system with OAS schemes while considering a single user is obtained, respectively. The secrecy diversity order of two-user MISO NOMA system for these two cases is obtained as $G_d^{\text{OAS},1} = G_d^{\text{OAS},2} = 0$.

D. MISO NOMA SYSTEMS WITH STT SCHEME

When $\lambda_{D_2} \to \infty$ and $\lambda_{D_1} = \beta\lambda_{D_2}$, we have

$$F_{\gamma_{D_1}}^{\infty,\mathrm{STT}}(\gamma) = \frac{{N_S}^{N_S}\gamma^{N_S}}{\left(\beta\lambda_{D_2}a_1\rho\right)^{N_S}}, \tag{51}$$

$$F_{\gamma_{D_2}}^{\infty,\mathrm{STT}}(\gamma) = \begin{cases} \dfrac{{N_S}^{N_S}\gamma^{N_S}}{\left(\lambda_{D_2}\rho\left(a_2 - a_1\gamma\right)\right)^{N_S}}, & \gamma < \dfrac{a_2}{a_1} \\ 1, & \gamma \geq \dfrac{a_2}{a_1}. \end{cases} \tag{52}$$

Utilizing (33), (51), and [34, eq. (3.351.3)], we obtain

$$\begin{aligned} P_{out,D_1}^{\infty,\mathrm{STT}} &= \int_0^\infty F_{\gamma_{D_1}}^{\infty,\mathrm{STT}}\left(\Theta_1(1+\gamma)-1\right) f_{\gamma_{E_1}}^{\mathrm{STT}}(\gamma)d\gamma \\ &= \frac{{N_S}^{N_S+2}}{\lambda_E a_1\rho\left(\beta\lambda_{D_2}a_1\rho\right)^{N_S}} \sum_{i=0}^{N_S-1}\sum_{k=0}^{N_S}\int_0^\infty \gamma^k e^{-\frac{(i+1)N_S\gamma}{\lambda_E a_1\rho}}d\gamma \\ &\quad \times \frac{(-1)^i\left(N_S-1\right)!}{i!\left(N_S-1-i\right)!}\frac{N_S!(\Theta_1-1)^{N_S-k}{\Theta_1}^k}{k!\left(N_S-k\right)!} \\ &= \frac{(N_S-1)!N_S!}{\beta^{N_S}{\lambda_{D_2}}^{N_S}} \sum_{i=0}^{N_S-1}\sum_{k=0}^{N_S}\frac{(-1)^i{N_S}^{N_S-k+1}}{i!\left(N_S-1-i\right)!} \\ &\quad \times \frac{(\Theta_1-1)^{N_S-k}(\Theta_1\lambda_E)^k\Gamma\left(k+1\right)}{k!\left(N_S-k\right)!(i+1)^{k+1}(a_1\rho)^{N_S-k}}. \end{aligned} \tag{53}$$

Using (34), (52), and Gaussian-Chebyshev quadrature method, we obtain

$$\begin{aligned} &P_{out,D_2}^{\infty,\mathrm{STT}} \\ &= \int_0^\infty F_{\gamma_{D_2}}^{\infty,\mathrm{STT}}\left(\Theta_2\left(1+\gamma\right)-1\right) f_{\gamma_{E_2}}^{\mathrm{STT}}(\gamma)\,d\gamma \\ &= I_2^{\mathrm{STT}} + \frac{a_2{N_S}^{N_S+2}}{\lambda_E\rho^{N_S+1}{\lambda_{D_2}}^{N_S}} \sum_{j=0}^{N_S-1}\frac{(-1)^j\left(N_S-1\right)!}{j!\left(N_S-1-j\right)!} \\ &\quad \times \int_0^\infty \frac{\left(\Theta_2\left(1+\gamma\right)-1\right)^{N_S}e^{-\frac{N_S(j+1)\gamma}{\lambda_E\rho(a_2-a_1\gamma)}}d\gamma}{\left(\lambda_{D_2}\rho(a_2-a_1(\Theta_2(1+\gamma)-1))\right)^{N_S}(a_2-a_1\gamma)^2} \\ &= I_2^{\mathrm{STT}} + \Xi_2\sum_{j=0}^{N_S-1}\sum_{n=1}^{N}\frac{(-1)^j}{j!\left(N_S-1-j\right)!} \\ &\quad \times \frac{\sqrt{1-\tau_n{}^2}(\Theta_2\vartheta_n+\Theta_2-1)^{N_S}e^{-\frac{N_S(j+1)\vartheta_n}{\lambda_E\rho(a_2-a_1\vartheta_n)}}}{\left(a_2-a_1\left(\Theta_2\vartheta_n+\Theta_2-1\right)\right)^{N_S}\left(a_2-a_1\vartheta_n\right)^2}, \end{aligned} \tag{54}$$

where $\Xi_2 = \frac{a_2\varpi\pi{N_S}^{N_S+2}(N_S-1)!}{2N\lambda_E\rho^{N_S+1}{\lambda_{D_2}}^{N_S}}$.

Substituting (53) and (54) into (40), the asymptotic SOP for MISO NOMA system with STT scheme is obtained. One can obtain the secrecy diversity order of the near and far users in this case as N_S and 0, respectively. That is to say, the diversity order of two-user MISO NOMA system with STT scheme is 0.

Remark 3: Observing the obtained analytical results above, one can deduce that the diversity order of all the TAS schemes is zero. This is because the diversity order of the far user is zero with the fixed power allocation scheme, which determines the diversity order of two-user NOMA system.

VI. A POWER ALLOCATION METHOD TO ACHIEVE NON-ZERO DIVERSITY ORDER

In this subsection, a new variable power allocation method is proposed to achieve non-zero diversity order.

Let $\frac{a_2}{a_1} = \alpha{\lambda_{D_2}}^{\varphi}$ $(0<\varphi<1)$ $(\alpha>0)$. Considering $a_2 + a_1 = 1$, we can obtain

$$\begin{cases} a_1 = \dfrac{1}{1+\alpha{\lambda_{D_2}}^{\varphi}} \\ a_2 = \dfrac{\alpha{\lambda_{D_2}}^{\varphi}}{1+\alpha{\lambda_{D_2}}^{\varphi}}. \end{cases} \tag{55}$$

A. SISO NOMA SYSTEMS

Utilizing (5), (55), and $e^x = \sum_{m=0}^{k}\frac{x^m}{m!} + \mathcal{O}\left(x^k\right)$, we obtain $F_{\gamma_{D_2}}^{\infty}(\gamma)$ as

$$F_{\gamma_{D_2}}^{\infty}(\gamma) = \frac{\gamma}{a_2\rho\lambda_{D_2}}. \tag{56}$$

When $\lambda_{D_2} \to \infty$, the instantaneous SINR of the eavesdropper eavesdropping the transmitted signal at the receiver D_2 can be given as

$$\gamma_{E_2} = \frac{|h_E|^2a_2}{|h_E|^2a_1 + \frac{1}{\rho}} \approx a_2\rho|h_E|^2. \tag{57}$$

Based on (57), the PDF of the eavesdropper applicable to the new power allocation method can written as

$$f_{\gamma_{E_2}}^{\mathrm{non}}(\gamma) = \frac{1}{a_2\rho\lambda_E}e^{-\frac{\gamma}{a_2\rho\lambda_E}}. \tag{58}$$

Substituting (55) into (44), we obtain the asymptotic SOP at D_1 as

$$P_{out,D_1}^{\infty} = \frac{\left(1+\alpha{\lambda_{D_2}}^{\varphi}\right)(\Theta_1-1)+\rho\lambda_E\Theta_1}{\beta\lambda_{D_2}\rho}. \tag{59}$$

Substituting (56) and (58) into (9) and making use of [34, eq. (3.381.4)], we obtain

$$P_{out,D_2}^{\infty} = \frac{\Theta_2a_2\rho\lambda_E+\Theta_2-1}{a_2\rho\lambda_{D_2}}. \tag{60}$$

From (59) and (60), one can easily obtain the diversity order for two users with the proposed power allocation scheme is $1-\varphi$ and 1, respectively. This means the diversity order of the far user increases by decreasing the diversity order of the near user. Thus, the secrecy diversity order of two-user NOMA is improved by

$$G_d^{\mathrm{SISO}} = 1-\varphi. \tag{61}$$

Remark 4: The power allocation scheme proposed in this paper is able to recover the diversity order by balancing the diversity gain of the near user and the diversity gain of the far user based on the channel gains.

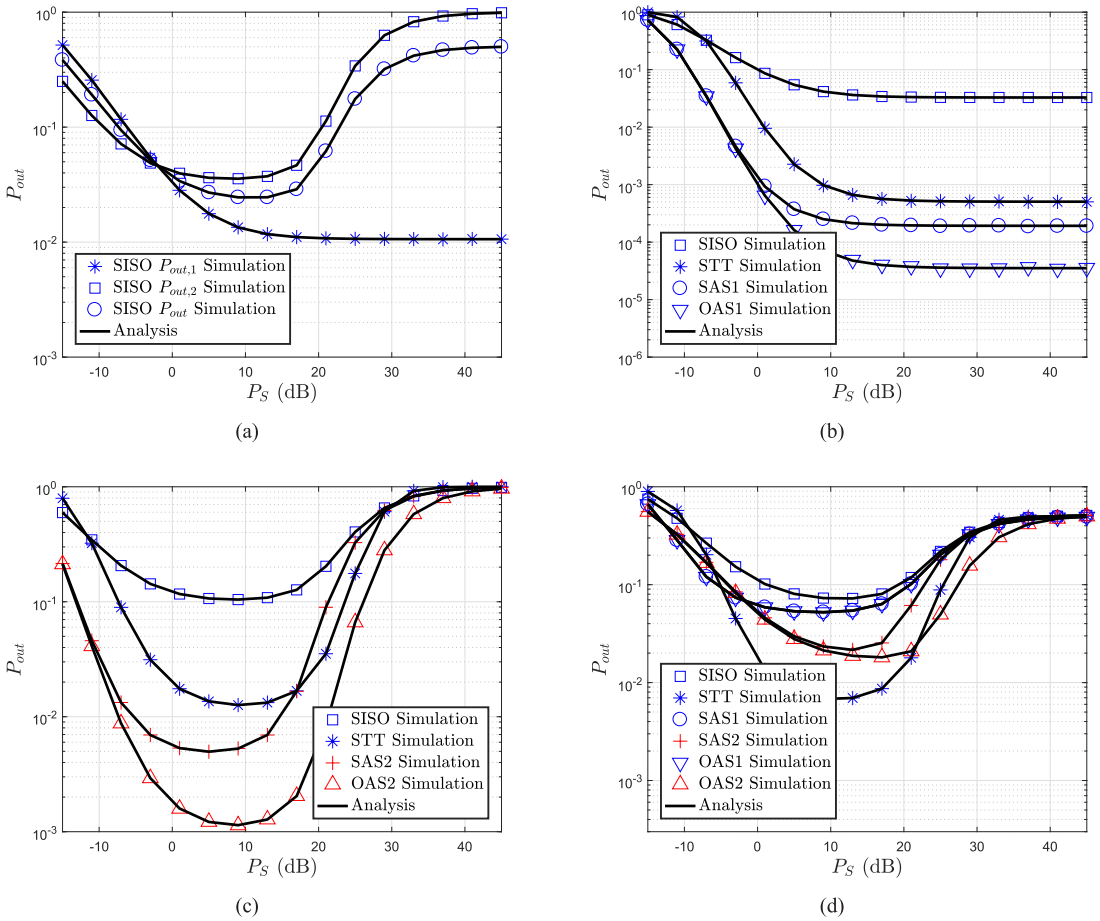

FIGURE 2. SOP for various P_S with $\lambda_{D_1} = 15$ dB, $\lambda_{D_2} = 10$ dB, $\lambda_E = -5$ dB, $a_1 = 0.1$, and $a_2 = 0.9$. (a) SOP of a SISO NOMA system. (b) SOP for D_1. (c) SOP for D_2. (d) SOP for the two-user NOMA system.

B. MISO NOMA SYSTEMS WITH SAS SCHEME

Utilizing (55) into (25), and $e^x = \sum_{m=0}^{k} \frac{x^m}{m!} + \mathcal{O}\left(x^k\right)$, we obtain

$$F_{\gamma_{D_2}}^{\infty,\mathrm{SAS}}(\gamma) = \frac{\gamma^{N_S}}{\left(a_2 \rho \lambda_{D_2}\right)^{N_S}}. \tag{62}$$

Substituting (55) into (48), we obtain the asymptotic SOP at D_1 as

$$P_{out,D_1}^{\infty,\mathrm{SAS}} = \sum_{k=0}^{N_S} \frac{N_S! \Theta_1^k (\Theta_1 - 1)^{N_S-k} {\lambda_E}^k \left(1 + \alpha \lambda_{D_2}{}^{\varphi}\right)^{N_S-k}}{(N_S - k)! \beta^{N_S} {\lambda_{D_2}}^{N_S} (\rho)^{N_S-k}}. \tag{63}$$

Substituting (62) and (58) into (9) and making use of [34, eq. (3.381.4)], we obtain

$$\begin{aligned} P_{out,D_2}^{\infty,\mathrm{SAS}} &= \frac{N_S!}{\left(\lambda_{D_2} \rho a_2\right)^{N_S} \lambda_E \rho a_2} \\ &\quad \times \sum_{k=0}^{N_S} \frac{(\Theta_2 - 1)^{N_S-k} \Theta_2{}^k}{k!\,(N_S - k)!} \int_0^{\infty} \gamma^k e^{-\frac{\gamma}{\lambda_E \rho a_2}} d\gamma \\ &= \frac{N_S!}{{\lambda_{D_2}}^{N_S}} \sum_{k=0}^{N_S} \frac{(\Theta_2 - 1)^{N_S-k} \Theta_2{}^k {\lambda_E}^k}{(N_S - k)! (\rho a_2)^{N_S-k}}. \end{aligned} \tag{64}$$

Based on (63), we easily obtain the diversity order for D_1 with SAS scheme considering D_1 as $(1-\varphi)N_S$. Similarly, the diversity order for D_2 with SAS scheme considering D_2 is obtained as N_S from (64). Note that the SOP for D_2 with SAS scheme considering D_1 is the same as D_2 in SISO scenario, and the SOP for D_1 with SAS scheme considering D_2 is the same as D_1 in SISO scenario. Thus, the diversity order of the two-user MISO NOMA system with SAS scheme under the proposed power allocation scheme is

$$G_d^{\mathrm{SAS},1} = \min\{(1-\varphi)N_S, 1\}, \tag{65}$$

$$G_d^{\mathrm{SAS},2} = 1 - \varphi, \tag{66}$$

respectively.

C. MISO NOMA SYSTEMS WITH OAS SCHEME

Based on (19), we can easily obtain the diversity order for the two users with OAS scheme scenario as $(1-\varphi)N_S$ and N_S, respectively. Note that the SOP for D_2 with OAS scheme considering D_1 is the same as D_2 in SISO scenario, and the SOP for D_1 with OAS scheme considering D_2 is the same as D_1 in SISO scenario. Finally, we obtain the diversity order for the two-user MISO NOMA system with OAS scheme

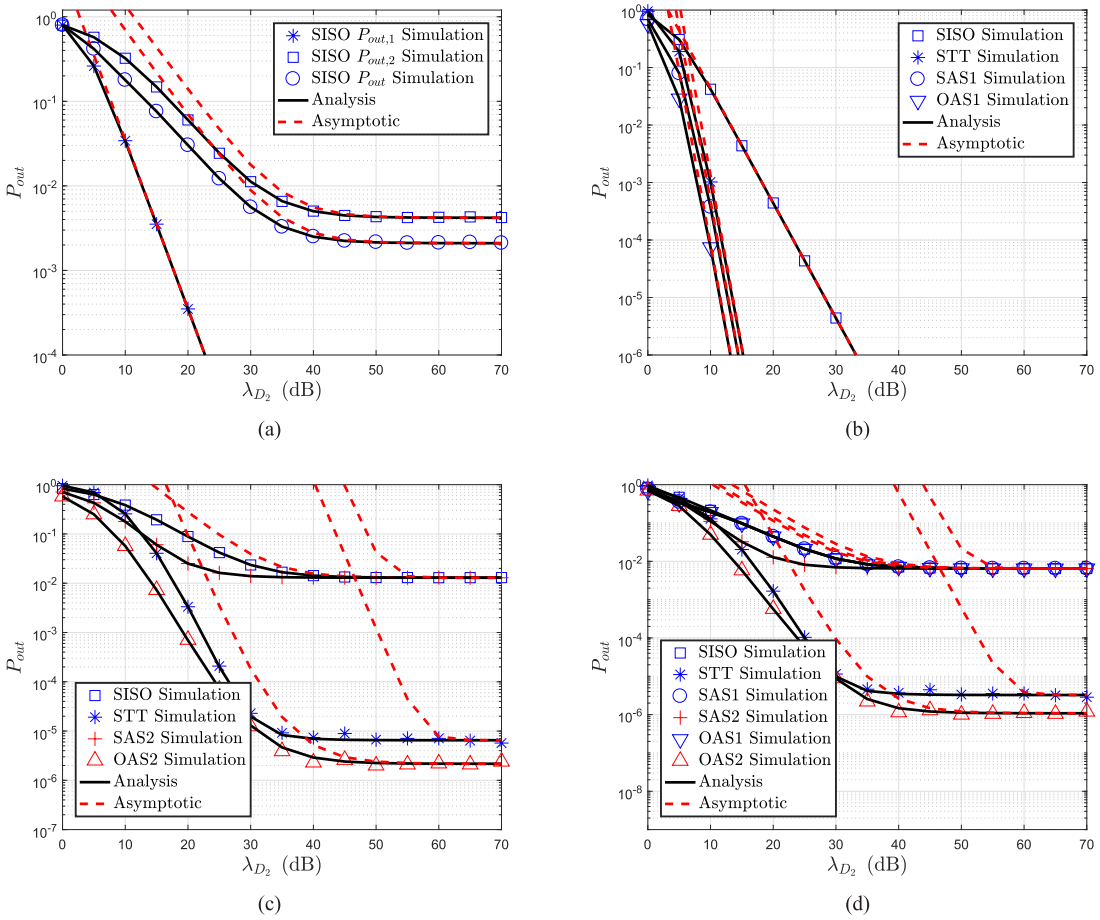

FIGURE 3. SOP for various λ_{D_2} with $\lambda_E = 5$ dB, $N_S = 3$, $a_1 = 0.1$, $a_2 = 0.9$, $\beta = 1.2$, and $P_S = 10$ dB. (a) SOP of a SISO NOMA system. (b) SOP for D_1. (c) SOP for D_2. (d) SOP for the two-user NOMA system.

under the proposed power allocation scheme as

$$G_d^{\mathrm{OAS},1} = \min\left\{(1-\varphi)N_S, 1\right\}, \tag{67}$$

$$G_d^{\mathrm{OAS},2} = 1-\varphi, \tag{68}$$

Remark 5: It should be noted that the SAS/OAS considering the near user is more beneficial in terms of diversity gain, which means $G_d^1 > G_d^2$.

D. MISO NOMA SYSTEMS WITH STT SCHEME

By substituting (55) into (32), and $e^x = \sum_{m=0}^{k} \frac{x^m}{m!} + \mathcal{O}\left(x^k\right)$, we obtain

$$F_{\gamma_{D_2}}^{\infty,\mathrm{STT}}(\gamma) = \frac{{N_S}^{N_S}\gamma^{N_S}}{\left(\lambda_{D_2}\rho a_2\right)^{N_S}}. \tag{69}$$

Similarly, the $f_{\gamma_{k_2}}^{\mathrm{STT,non}}(\gamma)$ can be rewritten as

$$f_{\gamma_{k_2}}^{\mathrm{STT,non}}(\gamma) = \frac{{N_S}^2}{\lambda_E \rho a_2}\sum_{i=0}^{N_S-1}\frac{(-1)^i(N_S-1)!}{i!(N_S-1-i)!}e^{-\frac{(i+1)N_S\gamma}{\lambda_E\rho a_2}}. \tag{70}$$

Substituting (55) into (53), we obtain

$$P_{out,D_1}^{\infty,\mathrm{STT}} = \sum_{i=0}^{N_S-1}\sum_{k=0}^{N_S}\frac{(-1)^i(N_S-1)!N_S!{N_S}^{N_S-k+1}}{i!(N_S-1-i)!(N_S-k)!} \times \frac{(\Theta_1-1)^{N_S-k}(\Theta_1\lambda_E)^k\left(1+\alpha\lambda_{D_2}\varphi\right)^{N_S-k}}{(i+1)^{k+1}\beta^{N_S}{\lambda_{D_2}}^{N_S}\rho^{N_S-k}}. \tag{71}$$

On substituting (69) and (70) into (9) and making use of [34, eq. (3.381.4)], we obtain

$$\begin{aligned} P_{out,D_2}^{\infty,\mathrm{STT}} &= \frac{{N_S}^{N_S+2}}{\left(\lambda_{D_2}\rho a_2\right)^{N_S}\lambda_E\rho a_2}\sum_{k=0}^{N_S}\sum_{i=0}^{N_S-1}\frac{N_S!(\Theta_2-1)^{N_S-k}}{k!(N_S-k)!} \\ &\quad\times\frac{(-1)^i(N_S-1)!{\Theta_2}^k}{i!(N_S-1-i)!}\int_0^\infty \gamma^k e^{-\frac{(i+1)N_S\gamma}{\lambda_E\rho a_2}}d\gamma \\ &= \frac{N_S!(N_S-1)!}{\left(\lambda_{D_2}\rho a_2\right)^{N_S}}\sum_{k=0}^{N_S}\sum_{i=0}^{N_S-1}\frac{(-1)^i(\lambda_E\rho a_2\Theta_2)^k}{(N_S-k)!i!} \\ &\quad\times\frac{{N_S}^{N_S-k+1}(\Theta_2-1)^{N_S-k}}{(N_S-1-i)!(i+1)^{k+1}}. \end{aligned} \tag{72}$$

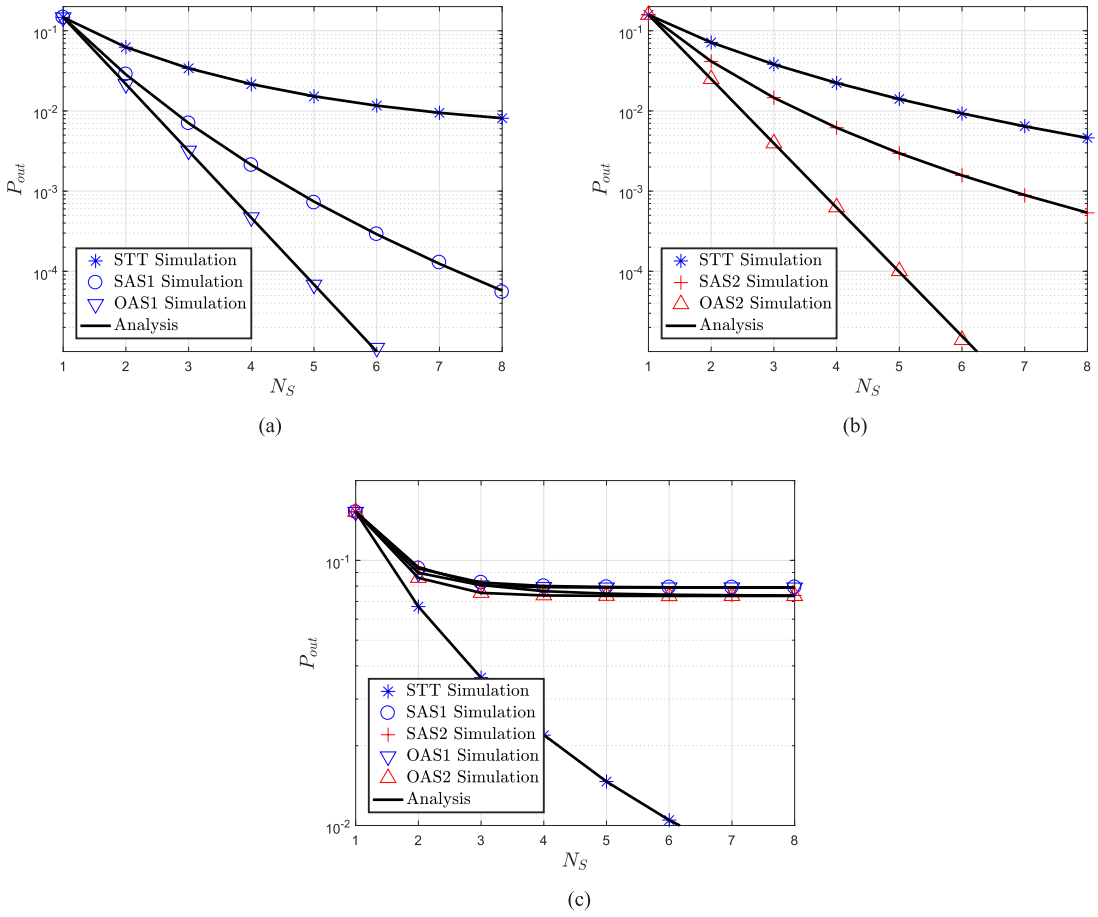

FIGURE 4. SOP for various N_S with $\lambda_{D_1} = 10$ dB, $\lambda_{D_2} = 8$ dB, $\lambda_E = 0$ dB, $a_1 = 0.1$, $a_2 = 0.9$, and $P_S = 5$ dB. (a) SOP for D_1. (b) SOP for D_2. (c) SOP for the two-user NOMA system.

Similarly, the diversity order for the two users with STT scheme is easily obtained as $(1-\varphi)N_S$ and N_S, respectively. Finally we obtain the diversity order of MISO NOMA system with STT scheme as

$$G_d^{\text{STT}} = (1-\varphi)N_S. \tag{73}$$

VII. NUMERICAL RESULTS AND DISCUSSIONS

In this section, the proposed analytical models are verified via Monte-Carlo simulation. The main parameters utilized in the simulations are set as $R_{s,1} = R_{s,2} = 0.1$ bit/s/Hz, $\sigma^2 = 1$. In all the figures, 'SAS1' and 'SAS2' means the SAS scheme based on D_1 or D_2, respectively. Similarly 'OAS1' and 'OAS2' means the OAS scheme based on D_1 or D_2, respectively.

Fig. 2 depicts the SOP versus P_S, where Figs. 2(a), 2(b), 2(c), and 2(d) plot the SOP for a SISO NOMA system, the SOP for D_1, D_2, and the two-user NOMA system with different TAS schemes, respectively. One can observe from Fig. 2(a) that the SOP at D_1 is improved until it reaches a floor. The reason is that the secrecy capacity tends to a constant when P_S becomes large [35]. An interesting result is found that the SOP at D_2 degrades before it reaches a ceil because the interference from D_1 increases while P_S increasing, which testifies the result in *Remark 1*. Further, the SOP at D_2 is superior to that at D_1 in the low transmit power region although the channel quality of S-D_1 is better than that of S-D_2. This is because physical layer security utilizes the randomness of the wireless channel. However, the SOP at D_2 gets worse in the high transmit power region until it reaches a constant due to increasing interference from D_1. The SOP of the NOMA system deteriorates due to the increase of the SOP at D_2. Figs. 2(b) and 2(c) depict the SOP for D_1 and D_2 with different TAS schemes versus P_S. One can observe that multiple antennas can improve the secrecy outage performance and the SOPs of SAS and OAS schemes outperform the STT scheme for both users. In Fig. 2(d), it can be observed that the SOP for NOMA system with STT outperforms those with SAS and OAS schemes. This is because in the SAS1 and OAS1 schemes only D_1 is considered in selecting transmit antenna. Since one transmit antenna is selected randomly for D_2, the SOP for D_2 with SAS1 and OAS1 schemes is the same as the case with a single antenna at S.

Fig. 3 depicts the SOP versus λ_{D_2}. One can observe that the asymptotic curves tightly approximate the exact ones as

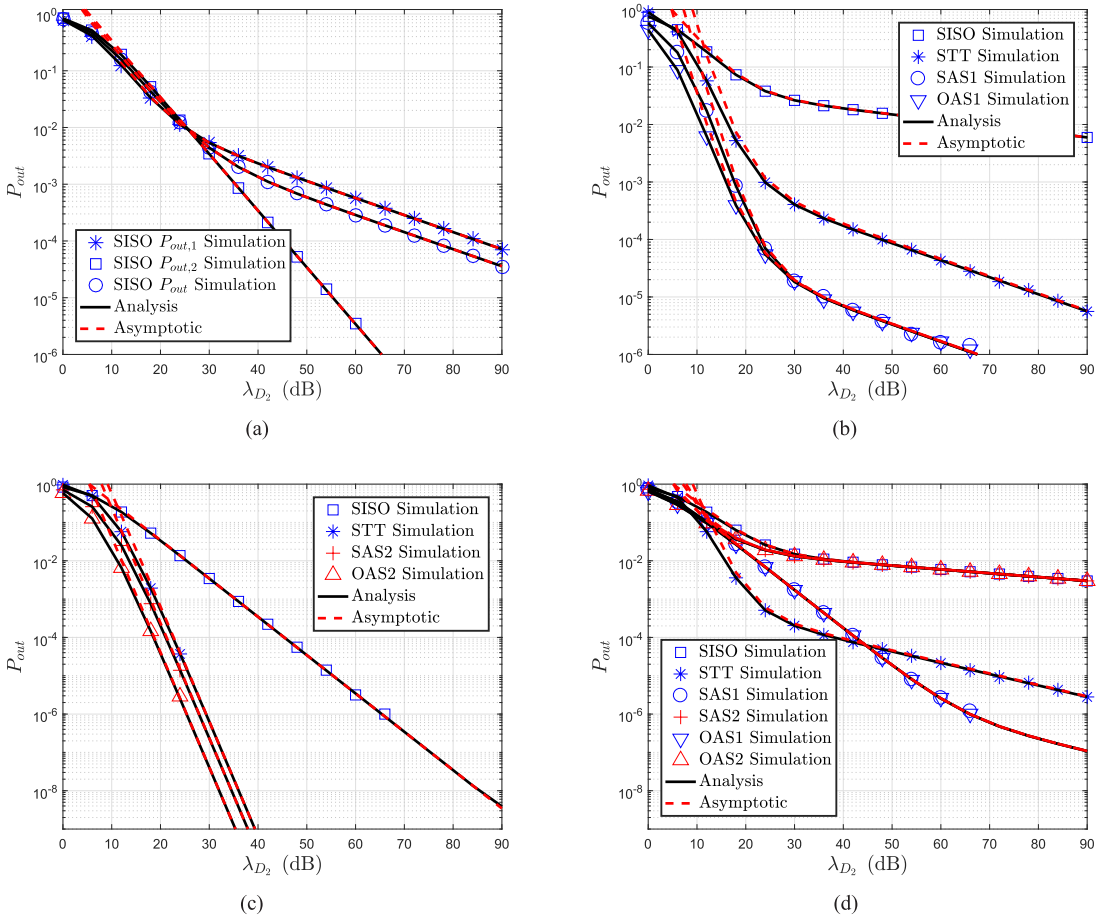

FIGURE 5. SOP with the proposed power allocation scheme for various λ_{D_2} with $\lambda_E = 3$ dB, $N_S = 3$, $\beta = 2$, $\alpha = 1.5$, $\varphi = 0.9$, and $P_S = 10$ dB. (a) SOP of a SISO NOMA system. (b) SOP for D_1. (c) SOP for D_2. (d) SOP for the two-user NOMA system.

λ_{D_2} increases. The SOP of NOMA system is determined by the farther user and hence the SOP of SISO NOMA system reaches a constant when λ_{D_2} tends to infinity. Thus the diversity order of SISO NOMA system is zero. Moreover, similar results can be observed from Figs. 3(c) and 3(d).

Figs. 4 depicts the SOP for MISO NOMA system with different TAS schemes versus N_S. It is observed from Figs. 4(a) and 4(b) that multiple antennas can improve the secrecy outage performance of each user when OAS scheme is considered in selecting antenna. From Fig. (c), it is found that the SOP of the NOMA system with SAS scheme is not affected by the number of the antennas when $N_S > 3$ whereas the NOMA system with STT scheme is effected. This means that increasing the antenna number hardly affects the secrecy performance of the NOMA system with TAS scheme but improves with the STT scheme.

Figs. 5 plots the SOP for SISO and MISO NOMA systems with the proposed power allocation scheme. We can observe that the non-zero diversity order is obtained for all the cases. We see in Figs. 5(a), 5(b), and 5(c) that the diversity order of NOMA system can be improved by decreasing the diversity order of the farther user. Fig. 5(d) demonstrates all the cases with the proposed power allocation scheme. We can observe that in SAS2 and OAS2 schemes, since $P_{out,D_2}^{\infty,\mathrm{SAS}}$ and $P_{out,D_2}^{\infty,\mathrm{OAS}}$ is very small (can be found in Fig. 5(c)), then the SOP of D_1 in SAS2 and OAS2 are dominant part of the SOP for the NOMA system (the SOP of D_1 in SAS2 and OAS2 are same as ones in SISO in Fig. 5(b)). So there is almost no difference between the SOP of SISO, SAS2, and OAS2 schemes. Similarly, from Fig. 5(c), one can observe that $P_{out,D_1}^{\infty,\mathrm{SAS}}$ and $P_{out,D_1}^{\infty,\mathrm{OAS}}$ is small (Fig. 5(b)) and the SOP of D_2 in SAS1 and OAS1 schemes are dominant part of the SOP for the NOMA system (the SOP of D_2 in SAS1 and OAS1 schemes are same as the ones in SISO in Fig. 5(c)). Furthermore, we can observe that the SOP with SAS1 and OAS1 schemes outperform STT scheme scenario with the proposed power allocation method in the high SNR regime.

VIII. CONCLUSION

In this work, the secrecy outage performance of two-user SISO and MISO NOMA systems with different TAS schemes was investigated. The exact and approximated closed-form expressions of the SOP for different TAS schemes were derived and compared with the one of traditional

STT scheme. The proposed analytical results were verified via Monte-Carlo simulations. The results demonstrate that the diversity order is zero when the fixed power allocation scheme is utilized. Subsequently, an effective power allocation strategy has been proposed and the diversity order achieved by the proposed power allocation scheme was analyzed.

ACKNOWLEDGMENT

The authors would like to thank the Editor and anonymous reviewers for their helpful comments and suggestions in improving the quality of this paper.

REFERENCES

[1] Z. Ding *et al.*, "Application of non-orthogonal multiple access in LTE and 5G networks," *IEEE Commun. Mag.*, vol. 55, no. 2, pp. 185–191, Feb. 2017.
[2] L. Dai, B. Wang, Y. Yuan, S. Han, C.-L. I, and Z. Wang, "Non-orthogonal multiple access for 5G: Solutions, challenges, opportunities, and future research trends," *IEEE Commun. Mag.*, vol. 53, no. 9, pp. 74–81, Sep. 2015.
[3] Y. Saito, A. Benjebbour, Y. Kishiyama, and T. Nakamura, "System-level performance of downlink non-orthogonal multiple access (NOMA) under various environments," in *Proc. IEEE 81st Veh. Technol. Conf. (VTC Spring)*, Glasgow, Scotland, May 2015, pp. 1–5.
[4] Z. Ding, P. Fan, and H. V. Poor, "Impact of user pairing on 5G nonorthogonal multiple-access downlink transmissions," *IEEE Trans. Veh. Technol.*, vol. 65, no. 8, pp. 6010–6023, Aug. 2016.
[5] T. M. Cover and J. A. Thomas, *Elements of Information Theory*. Hoboken, NJ, USA: Wiley, 2012.
[6] Z. Ding, Z. Yang, P. Fan, and H. V. Poor, "On the performance of non-orthogonal multiple access in 5G systems with randomly deployed users," *IEEE Signal Process. Lett.*, vol. 21, no. 12, pp. 1501–1505, Dec. 2014.
[7] S. Timotheou and I. Krikidis, "Fairness for non-orthogonal multiple access in 5G systems," *IEEE Signal Process. Lett.*, vol. 22, no. 10, pp. 1647–1651, Oct. 2015.
[8] J. Cui, Z. Ding, and P. Fan, "A novel power allocation scheme under outage constraints in NOMA systems," *IEEE Signal Process. Lett.*, vol. 23, no. 9, pp. 1226–1230, Sep. 2016.
[9] Z. Yang, Z. Ding, P. Fan, and N. Al-Dhahir, "A general power allocation scheme to guarantee quality of service in downlink and uplink NOMA systems," *IEEE Trans. Wireless Commun.*, vol. 15, no. 11, pp. 7244–7257, Nov. 2016.
[10] S. M. R. Islam, N. Avazov, O. A. Dobre, and K. S. Kwak, "Power-domain non-orthogonal multiple access (NOMA) in 5G systems: Potentials and challenges," *IEEE Commun. Surveys Tuts.*, vol. 19, no. 2, pp. 721–742, 2nd Quart., 2017.
[11] Y. Liu, M. Elkashlan, Z. Ding, and G. K. Karagiannidis, "Fairness of user clustering in MIMO non-orthogonal multiple access systems," *IEEE Commun. Lett.*, vol. 20, no. 7, pp. 1465–1468, Jul. 2016.
[12] M. F. Hanif, Z. Ding, T. Ratnarajah, and G. K. Karagiannidis, "A minorization-maximization method for optimizing sum rate in the downlink of non-orthogonal multiple access systems," *IEEE Trans. Signal Process.*, vol. 64, no. 1, pp. 76–88, Jan. 2016.
[13] Y. Liu, Z. Ding, M. Elkashlan, and H. V. Poor, "Cooperative non-orthogonal multiple access with simultaneous wireless information and power transfer," *IEEE. J. Sel. Areas Commun.*, vol. 34, no. 4, pp. 938–953, Apr. 2016.
[14] Z. Ding, F. Adachi, and H. V. Poor, "The application of MIMO to non-orthogonal multiple access," *IEEE Trans. Wireless Commun.*, vol. 15, no. 1, pp. 537–552, Jan. 2016.
[15] Y. Liu, G. Pan, H. Zhang, and M. Song, "On the capacity comparison between MIMO-NOMA and MIMO-OMA," *IEEE Access*, vol. 4, pp. 2123–2129, May 2016.
[16] W. Han, J. Ge, and J. Men, "Performance analysis for NOMA energy harvesting relaying networks with transmit antenna selection and maximal-ratio combining over Nakagami-*m* fading," *IET Commun.*, vol. 10, no. 18, pp. 2687–2693, Dec. 2016.
[17] X. Liu and X. Wang, "Efficient antenna selection and user scheduling in 5G massive MIMO-NOMA system," in *Proc. IEEE 83rd Veh. Technol. Conf. (VTC Spring)*, Nanjing, China, May 2016, pp. 1–5.
[18] Y. Yu, H. Chen, Y. Li, Z. Ding, and B. Vucetic. (Dec. 2016). "Antenna selection for MIMO non-orthogonal multiple access systems." [Online]. Available: https://arxiv.org/abs/1612.04943
[19] J. Men and J. Ge, "Non-orthogonal multiple access for multiple-antenna relaying networks," *IEEE Commun. Lett.*, vol. 19, no. 10, pp. 1686–1689, Oct. 2015.
[20] J. Men, J. Ge, and C. Zhang, "Performance analysis of non-orthogonal multiple access for relaying networks over Nakagami-*m* fading channels," *IEEE Trans. Veh. Technol.*, vol. 66, no. 2, pp. 1200–1208, Feb. 2017.
[21] Z. Zhang, Z. Ma, M. Xiao, Z. Ding, and P. Fan, "Full-duplex device-to-device aided cooperative non-orthogonal multiple access," *IEEE Trans. Veh. Technol.*, vol. 66, no. 5, pp. 4467–4471, May 2016.
[22] Y. Liu, Z. Ding, M. Elkashlan, and J. Yuan, "Non-orthogonal multiple access in large-scale underlay cognitive radio networks," *IEEE Trans. Veh. Technol*, vol. 65, no. 12, pp. 10152–10157, Dec. 2016.
[23] F. Lu, M. Xu, L. Cheng, J. Wang, J. Zhang, and G. K. Chang, "Non-orthogonal multiple access with successive interference cancellation in millimeter-wave radio-over-fiber systems," *J. Lightw. Technol.*, vol. 34, no. 17, pp. 4179–4186, Sep. 2016.
[24] H. Marshoud, V. M. Kapinas, G. K. Karagiannidis, and S. Muhaidat, "Non-orthogonal multiple access for visible light communications," *IEEE Photon. Technol. Lett.*, vol. 28, no. 1, pp. 51–54, Jan. 2016.
[25] M. Bloch, J. Barros, M. R. D. Rodrigues, and S. W. McLaughlin, "Wireless information-theoretic security," *IEEE Trans. Inf. Theory*, vol. 54, no. 6, pp. 2515–2534, Jun. 2008.
[26] Y. Zhang, H. M. Wang, Q. Yang, and Z. Ding, "Secrecy sum rate maximization in non-orthogonal multiple access," *IEEE Commun. Lett.*, vol. 20, no. 5, pp. 930–933, May 2016.
[27] Z. Qin, Y. Liu, Z. Ding, Y. Gao, and M. Elkashlan, "Physical layer security for 5G non-orthogonal multiple access in large-scale networks," in *Proc. IEEE Int. Conf. Commun. (ICC)*, Kuala Lumpur, Malaysia, May 2016, pp. 1–6.
[28] Y. Liu, Z. Qin, M. Elkashlan, Y. Gao, and F. L. Hanzo, "Enhancing the physical layer security of non-orthogonal multiple access in large-scale networks," *IEEE Trans. Wireless Commun.*, vol. 16, no. 3, pp. 1656–1672, Mar. 2017.
[29] J. Zhu, Y. Zou, G. Wang, Y.-D. Yao, and G. K. Karagiannidis, "On secrecy performance of antenna-selection-aided MIMO systems against eavesdropping," *IEEE Trans. Veh. Technol.*, vol. 65, no. 1, pp. 214–225, Jan. 2016.
[30] H. Lei *et al.*, "Secrecy outage performance of transmit antenna selection for MIMO underlay cognitive radio systems over Nakagami-*m* channels," *IEEE Trans. Veh. Technol.*, vol. 66, no. 3, pp. 2237–2250, Mar. 2017.
[31] P. Xu, Z. Ding, X. Dai, and H. V. Poor, "A new evaluation criterion for non-orthogonal multiple access in 5G software defined networks," *IEEE Access*, vol. 3, pp. 1633–1639, Oct. 2015.
[32] Z. Ding, L. Dai, and H. V. Poor, "MIMO-NOMA design for small packet transmission in the Internet of Things," *IEEE Access*, vol. 4, pp. 1393–1405, Apr. 2016.
[33] Z. Ding, H. Dai, and H. V. Poor, "Relay selection for cooperative NOMA," *IEEE Wireless Commun. Lett.*, vol. 5, no. 4, pp. 416–419, Aug. 2016.
[34] I. S. Gradshteyn and I. M. Ryzhik, *Table of Integrals, Series and Products*, 7th. San Diego, CA, USA: Academic, 2007.
[35] H. Lei, I. S. Ansari, G. Pan, B. Alomair, and M.-S. Alouini, "Secrecy capacity analysis over $\alpha - \mu$ fading channels," *IEEE Commun. Lett.*, vol. 21, no. 6, pp. 1445–1448, Jun. 2017.
[36] M. Abramowitz and I. A. Stegun, *Handbook of Mathematical Functions With Formulas, Graphs, and Mathematical Tables*, 9th. New York, NY, USA: Dover, 1972.
[37] N. Yang, M. Elkashlan, P. L. Yeoh, and J. Yuan, "Multiuser MIMO relay networks in Nakagami-*m* fading channels," *IEEE Trans. Commun.*, vol. 60, no. 11, pp. 3298–3310, Nov. 2012.
[38] L. Wang, M. Elkashlan, J. Huang, R. Schober, and R. K. Mallik, "Secure transmission with antenna selection in MIMO Nakagami-*m* fading channels," *IEEE Trans. Wireless Commun.*, vol. 13, no. 11, pp. 6054–6067, Nov. 2014.
[39] H. Lei, M. Xu, I. S. Ansari, G. Pan, K. A. Qaraqe, and M.-S. Alouini, "On secure underlay MIMO cognitive radio networks with energy harvesting and transmit antenna selection," *IEEE Trans. Green Commun. Netw.*, vol. 1, no. 2, pp. 192–203, Jun. 2017.

HONGJIANG LEI (M'17) received the B.Sc. degree in mechanical and electrical engineering from the Shenyang Institute of Aeronautical Engineering, Shenyang, China, in 1998, the M.Sc. degree in computer application technology from Southwest Jiaotong University, Chengdu, China, in 2004, and the Ph.D. degree in instrument science and technology from Chongqing University, Chongqing, China, in 2015, respectively. In 2004, he joined the School of Communication and Information Engineering, Chongqing University of Posts and Telecommunications, Chongqing, China, where he is currently an Associate Professor. Since 2016, he has been with the Computer, Electrical, and Mathematical Science and Engineering Division, King Abdullah University of Science and Technology, Saudi Arabia, where he is currently a Post-Doctoral Research Fellow supported by the Chinese Scholarship Council. His research interest spans special topics in communications theory and signal processing, including physical layer security and cognitive radio networks. He is a TPC Member of IEEE Globecom'17. He has also served as a reviewer for major international journals, e.g., IEEE TVT, IEEE TCOM, IEEE TWC, IEEE TIFS, and IEEE CL.

JIANMING ZHANG received the B.Sc. degree in electrical engineering from the Hebei University of Architecture, Zhangjiakou, China, in 2015. He is currently pursuing the M.Sc. degree in information and communication engineering with the Chongqing University of Posts and Telecommunications, Chongqing, China. His research interests include cognitive radio networks, physical layer security, and non-orthogonal multiple access.

KI-HONG PARK (S'06–M'11) received the B.Sc. degree in electrical, electronic, and radio engineering from Korea University, Seoul, South Korea, in 2005, and the M.S. and Ph.D. degrees from the School of Electrical Engineering, Korea University, Seoul, South Korea, in 2011. Since 2011, he has been a Post-Doctoral Fellow of electrical engineering with the Division of Physical Science and Engineering, King Abdullah University of Science and Technology, Thuwal, Saudi Arabia. His research interests are broad in communication theory and its application to the design and performance evaluation of wireless communication systems and networks. On-going research includes the application to MIMO diversity/beamforming systems, cooperative relaying systems, physical layer secrecy, and optical wireless communications.

PENG XU received the B.Sc. and Ph.D. degrees in electronic and information engineering from the University of Science and Technology of China, Anhui, China, in 2009 and 2014, respectively. Since 2014, he has been a Post-Doctoral Researcher with the Department of Electronic Engineering and Information Science, University of Science and Technology of China, Hefei, China. Since 2016, he has been with the School of Communication and Information Engineering, Chongqing University of Posts and Telecommunications, Chongqing, China. His current research interests include cooperative communications, information theory, information-theoretic secrecy, and 5G networks. He received IEEE Wireless Communications Letters Exemplary Reviewer 2015.

IMRAN SHAFIQUE ANSARI (S'07–M'15) received the B.Sc. degree in computer engineering (Hons.) from the King Fahd University of Petroleum and Minerals in 2009 and the M.Sc. and Ph.D. degrees from the King Abdullah University of Science and Technology in 2010 and 2015, respectively. He is currently a Post-Doctoral Research Associate with Texas A&M University at Qatar. In 2009, he was a Visiting Scholar with Michigan State University, East Lansing, MI, USA, and from 2010 to 2010, he was a Research Intern with Carleton University, Ottawa, ON, Canada.

He has authored/co-authored more than 50 journal and conference publications. He has co-organized the GRASNET'2016 workshop in conjunction with IEEE WCNC'2016 and co-organizing the second edition GRASNET'2017 workshop in conjunction with IEEE WCNC'2017. His current research interests include free-space optics, channel modeling/signal propagation issues, relay/multihop communications, physical layer secrecy issues, full duplex systems, and diversity reception techniques among others.

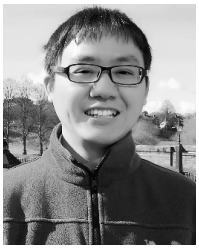

GAOFENG PAN (M'12) received the B.Sc. degree in communication engineering from Zhengzhou University, Zhengzhou, China, in 2005, and the Ph.D. degree in communication and information systems from Southwest Jiaotong University, Chengdu, China, in 2011. He was with The Ohio State University, Columbus, OH, USA, from 2009 to 2011, as a joint-trained Ph.D. student under the supervision of Prof. E. Ekici. In 2012, he joined the School of Electronic and Information Engineering, Southwest University, Chongqing, China, where he is currently an Associate Professor. Since 2016, he has also been with the School of Computing and Communications, Lancaster University, Lancaster, U.K., where he currently holds a postdoctoral position under the supervision of Prof. Z. Ding. His research interest spans special topics in communications theory, signal processing, and protocol design, including secure communications, CR communications, and MAC protocols. He is a TPC Member of IEEE Globecom'16 Workshop on Wireless Energy Harvesting Communication Networks. He has also served as a reviewer for major international journals, such as the IEEE TCOM, the IEEE TWC, the IEEE TSP, the IEEE TVT, the IEEE CL, and the IEEE WCL.

BASEL ALOMAIR (M'11) received the bachelor's degree from King Saud University, Riyadh, Saudi Arabia, the master's degree from the University of Wisconsin-Madison, Madison, WI, USA, and the Ph.D. degree from the University of Washington-Seattle, Seattle, WA, USA. He is currently an Assistant Professor and the Founding Director of the National Center for Cybersecurity Technology, King Abdulaziz City for Science and Technology, Riyadh, Saudi Arabia, an Affiliate Professor, and the Co-Director of the Network Security Laboratory, University of Washington-Seattle, an Affiliate Professor with King Saud University, and a cryptology consultant with various agencies.

Dr. Alomair was recognized by the IEEE Technical Committee on Fault-Tolerant Computing and the IFIP Working Group on Dependable Computing and Fault Tolerance (WG 10.4) with the 2010 IEEE/IFIP William Carter Award for his significant contributions in the area of dependable computing. He has authored/coauthored papers that received best paper awards. He was a recipient of the 2011 Outstanding Research Award from the University of Washington for his research in information security, the 2012 Distinguished Dissertation Award from the Center for Information Assurance and Cybersecurity at the University of Washington, and the 2015 Early Career Award in Cybersecurity by the NSA/DHS Center of Academic Excellence in Information Assurance Research for his contributions to Modern Cryptographic Systems and Visionary Leadership.

MOHAMED-SLIM ALOUINI (S'94–M'98–SM'03–F'09) was born in Tunis, Tunisia. He received the Ph.D. degree in Electrical Engineering from the California Institute of Technology, Pasadena, CA, USA, in 1998. He served as a Faculty Member with the University of Minnesota, Minneapolis, MN, USA, and then with the Texas A&M University at Qatar, Education City, Doha, Qatar, before joining the King Abdullah University of Science and Technology, Thuwal, Saudi Arabia, as a Professor of Electrical Engineering in 2009. His current research interests include the modeling, design, and performance analysis of wireless communication systems.